

Staging of osteochondral lesions of the talus: comparison of Cone Beam CT - Arthrography with Magnetic Resonance Imaging

Julie Desimpel^{1,2}, Filip M. Vanhoenacker^{1,2,3}

¹Department of Radiology, AZ Sint-Maarten, Mechelen, Belgium

²Department of Radiology, Antwerp University Hospital, Antwerp University, Belgium

³Faculty of Medicine and Health Sciences, Ghent University, Belgium

SUBMISSION: 24/2/2021 - ACCEPTANCE: 13/4/2021

ABSTRACT

Purpose: To evaluate the value of Cone Beam Computed Tomography (CBCT)-Arthrography (CBCT-A) versus Magnetic Resonance Imaging (MRI) for staging of osteochondral lesions of the talus.

Material and Methods: 35 consecutive patients with chronic ankle pain and an osteochondral lesion on MRI were included and subsequently underwent CBCT-A. The following parameters were analysed by two reviewers: size of lesion, depth of lesion, degree of detachment, presence of bone marrow oedema on 1.5 Tesla MRI or sclerosis on CBCT-A, presence of subchondral cysts and additional lesions in the tibia.

Results: Analysis of CBCT-Arthrography resulted in an upstaging in 17 patients with a statistically significant difference ($p < 0.05$) for the degree of detachment between MRI and CBCT-Arthrography.

Conclusions: CBCT-A allows a more precise staging of osteochondral lesion of the talus than 1.5 T MRI. However, because of its exposure to radiation and more invasive nature, MRI is recommended as the initial screening method for evaluation of osteochondral lesions of the ankle. Additional CBCT-A is reserved for selected cases in which surgical treatment is considered.



CORRESPONDING
AUTHOR,
GUARANTOR

Corresponding author: Dr. Julie Desimpel, Department of Radiology, AZ Sint-Maarten, Mechelen, Belgium, Antwerp University Hospital, Wilrijkstraat 102650 Edegem, Email: julie_desimpel@hotmail.com

Guarantor: Professor Dr. Filip Vanhoenacker, Department of Radiology, AZ Sint-Maarten, Mechelen, Belgium, Liersesteenweg 435 2800 Mechelen, Email: filip.vanhoenacker@telenet.be



KEY WORDS

Cone Beam CT; Musculoskeletal imaging; Ankle/talus; Arthrography; Magnetic Resonance Imaging; Osteochondral lesion

Introduction

An osteochondral lesion (OCL) is defined as any damage involving both articular cartilage and subchondral bone. The most common sites for OCL are the knee, ankle and elbow [1]. The underlying aetiology is variable. Most OCLs of the ankle are post-traumatic (due to a single high-energy trauma or due to repetitive micro-injuries) [2]. Accurate staging of the OCL is necessary to determine the treatment strategy for the best outcome. If unstable lesions are left untreated early osteoarthritis may develop.

Several imaging modalities can detect OCL of the ankle. Small lesions are often too small to detect on conventional radiographs (30 to 50% of the lesions are missed). Computed Tomography (CT) without intra-articular contrast has a high sensitivity for OCL (up to 0.81) but in comparison to MRI it doesn't allow evaluation of the cartilage [3]. The value of MDCT-Arthrography (CT-A) regarding staging of talar osteochondral lesions has been extensively described in the literature [4-7] but the potential added value of cone beam CT arthrography (CBCT-A) remains underreported. Kirsche et al. [5] reported the value of CT-A. The limitations of their study are the retrospective design and the relatively long time delay between the MDCT-A and MRI (mean time of 2.8 months) whilst our study had a prospective design and a limited time span between both examinations (mean time of 4 weeks). Although CBCT has been used to evaluate trauma of peripheral joints [8], a comparative study between CBCT following intra-articular injection of iodine contrast and MRI for evaluation of OCL of the talus has not been performed yet, which is the aim of our study.

Material and Methods

Our study has a prospective design. It has been approved by the Medical Ethical Committee of our institution (approval number EC1804). Written informed consent was obtained from all enrolled patients. We included 35 patients (20 male-15 female, aged 10-67 years-old, mean age 44, Standard Deviation 13.5) referred for MRI due

to chronic ankle pain and presenting with an OCL of the talus on MRI. There was an equal distribution of the affected side with 18 patients with an OCL in the right ankle and 17 patients with a left-sided lesion.

Exclusion criteria

Patients with previous ankle surgery and/or ankle implants were excluded from the study. All eligible patients subsequently underwent a CBCT-A.

MRI Imaging protocol

All MR examinations were performed on a 1.5T system (Siemens, Magnetom Aera, Erlangen, Germany) with a uniform standardised imaging protocol (sagittal, axial and coronal fat-suppressed (FS) T2-Weighted Images (WI) with intermediate weighting, coronal Proton Density (PD) and axial T1-WI with a slice thickness of 3 mm) (**Table 1**).

CBCT-A Imaging protocol

The contrast used for the CBCT-A examination was 10 cc Iohexol (Omnipaque, GE Healthcare, Chicago, Illinois, USA), 240mg I/ml diluted with 10 cc saline. A mean volume of 13 cc was intra-articularly injected by a 21 Gauge needle under fluoroscopic guidance. All CBCT-A examinations were performed on a New Tom 5G CBCT (QR systems, Verona, Italy) within 15 to 25 minutes after contrast injection. CBCT-A was performed within a time span of maximum 4 weeks following the MRI examination. Both examinations were conducted with the patient in supine position and feet pointing upwards.

Imaging analysis

All images were transferred on Picture Archiving Communication System (PACS) workstations (Agfa Enterprise, Mortsel, Belgium) for retrospective analysis and were independently evaluated by two reviewers: one senior radiologist with 31 years of experience (FMV) and one junior radiologist with 3 years of experience (JD). Both reviewers analysed the images twice with a twelve-week time gap in between. There were small discrepancies

Table 1. MRI protocol.

	FOV	TR	TE	Matrix
PD TSE Sag FS	185	3700	36	243x304
PD TSE Cor FS	160	3800	48	307x384
T1 TSE Trans	150	490	11	240x320
PD TSE Cor	160	2690	24	307x384
T2 TSE Trans FS	185	4020	39	307x384

FOV: Field Of View; TR: Repetition Time; TE: Echo Time, PD: Proton Density; TSE: Turbo Spin Echo; Sag: Sagittal; Cor: Coronal; Trans: Transversal; FS: Fat Suppressed

Table 2a. The modified Anderson classification.

Stage	Description	Diagram
Stage 1	subchondral trabecular compression; plain radiographs normal but positive bone scan, BME on MRI	
Stage 2a	formation of subchondral cyst and surrounding BME	
Stage 2b	incomplete separation of fragment, note surrounding BME	
Stage 3	completely detached, undisplaced fragment with presence of synovial fluid (around fragment and surrounding BME)	
Stage 4	displaced fragment with adjacent BME	

The modified Anderson classification evaluates the cartilage (blue) component (flap formation and delamination) and the subchondral bone (black) involvement (bone marrow edema (BME) on MRI or sclerosis on CBCT-A and cyst formation). The talocrural ligaments (orange) are intact. (Used with permission from [11])

Table 2b. The modified Outerbridge classification.

	MR IMAGING	ARTHROSCOPY	MACROSCOPY	SCHEMATIC DRAWING OF THE ARTICULAR CARTILAGE
Grade 0	homogenous and smooth delineation	uniform thickness and intact surface	normal cartilage	
Grade 1	focal areas of hyperintensity with normal contour	softening or swelling of cartilage	focal thickening	
Grade 2	blister-like swelling/fraying of articular cartilage extending to the surface	fragmentation and fissuring within soft areas of articular cartilage	superficial defect(s), less than 50%	
Grade 3	partial thickness cartilage loss with focal ulceration	partial thickness cartilage loss with fibrillation ("crab-meat appearance")	Deep defect(s) more than 50%	
Grade 4	exposed subchondral bone	cartilage destruction with exposed subchondral bone	Full thickness defect(s)	

The modified Outerbridge classification was used for the grading of the depth of the cartilage lesions. This Outerbridge classification system is widely used for staging of cartilage lesions of the knee. (Used with permission from [11]).

among both reviewers in one case for which the findings were reviewed in consensus. The following parameters were analysed: size of the lesion, depth of the cartilage defect, degree of cartilage detachment, presence of bone marrow oedema (BME) on MRI or subchondral sclerosis on CBCT-A, presence of subchondral cysts and additional lesions at the talus, tibia or fibula. The imaging parameters are a combination of two classifications consisting

of the modified Anderson classification [9] and the Outerbridge classification [10] (Tables 2a, 2b). The size of the lesion was measured in anteroposterior (AP) (measured on the axial T1-WI) and mediolateral (ML) (measured on the coronal PD images) directions. The depth of the lesion was categorised from 0 to 4. Grade 0 correlates with an intact cartilage. Grade 1 corresponds to a small superficial defect. In case of a grade 2 lesion the cartilage

Table 3. AP and ML size intra-rater variability.

	MRI		CBCT	
	Junior ICC _{intra}	Senior ICC _{intra}	Junior ICC _{intra}	Senior ICC _{intra}
AP size	0.916	0.916	0.930	0.974
ML size	0.832	0.982	0.875	0.921

Table 4. AP and ML size inter-rater variability.

	MRI		CBCT	
	Junior ICC _{inter}	Senior ICC _{inter}	Junior ICC _{inter}	Senior ICC _{inter}
AP size	0.915	0.980	0.997	0.999
ML size	0.874	0.832	0.915	0.996

Table 5. Depth of the cartilage lesion on MRI versus CBCT-A.

		Depth CBCT-A				
		0	1	2	3	4
Depth MRI	0	4	0	0	0	3
	1	1	0	0	0	1
	2	2	0	1	0	1
	3	0	0	0	0	0
	4	0	0	0	0	21

The grading of the depth of the OCL lesion on CBCT-A versus MRI was unchanged in 26 patients (numbers in bold on the diagonal line). We noted an upstaging in 5 patients (in green, above the diagonal line) and a downstaging in 3 patients (in red, below the diagonal line). There was 1 patient in which the depth was not assessable on MRI.

defect is less than 50%. Grade 3 lesions have a defect of more than 50%. Full thickness cartilage defect is graded as a grade 4 lesion. The degree of detachment was classified in no (0), partial (1) or complete (2) detachment.

Statistical methods

All statistical processing was performed with Statistical Package for Social Sciences (SPSS). Variables are summarised using mean and standard deviation for

Table 6. Degree of detachment on MRI versus CBCT-A.

		Detachment CBCT-A		
		0	1	2
Det. MRI	0	8	4	2
	1	1	8	10
	2	0	0	2

The degree of detachment was classified in no (0), partial (1) or complete (2) detachment. There was an upstaging of the degree of detachment in 16 patients on CBCT-A (in green, above the diagonal line). There was only one case in which the degree of detachment was downstaged on CBCT-A (in red, below the diagonal line). Our study showed a statistically significant difference between MRI and CBCT-A, p=0.003.

Table 7. Additional cartilage lesions on MRI versus CBCT-A.

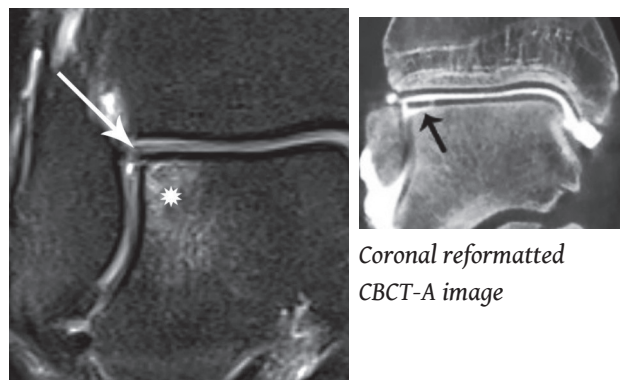
		Add. CBCT-A	
		0	1
Add. MRI	0	25	2
	1	0	8

CBCT-A revealed an additional cartilage lesions of the talus or tibia in two patients (in green).

Table 8. Advantages of CBCT in comparison to CT.

- ✓ Higher spatial resolution
- ✓ Lower radiation dose
- ✓ Lower installation cost
- ✓ Compact design
- ✓ Decreases the MDCT workload

continuous variables, and numbers and percentages for categorical variables. The results of the first measurement of the senior radiologist are reported. Normality of continuous variables was checked using QQ-plots and Shapiro-Wilk test. Continuous variables were compared between MRI and CBCT-A with paired T-test, for categorical variables McNemar test was used. The inter- and intra- rater variability for MRI and CBCT-A were assessed using intra-class correlation (ICC) with two-way



Coronal Intermediate-W MRI image

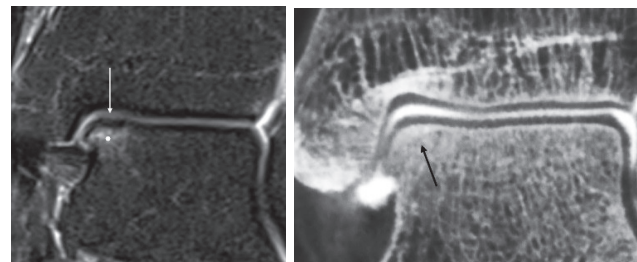
Fig 1. Example of upstaging of an OCL on CBCT-A compared to MRI. The coronal MRI image shows BME (white asterisk) at the lateral corner of the talar dome. Note also a slight irregular delineation of the cartilage (white arrow) at this site. CBCT-A shows almost complete detachment of the cartilage at the superolateral aspect of the talar dome (black arrow).

ANOVA with random effects. Agreement between MRI and CBCT-A for categorical variables was assessed using kappa-statistics.

Results

The mean AP size of the OCL lesions on MRI was 9.5 mm (range 1.5-16 mm). The mean AP size of the OCL lesions on CBCT-A was 9 mm (range 2-16.5 mm). The mean ML size of the OCL lesions on MRI was 7 mm (range 2-11 mm). The mean ML size of the OCL lesions on CBCT-A was 7.3 mm (range 2-13 mm). There was no statistical significant difference in size between both imaging modalities. The intra-rater variability and inter-rater variability of both the AP and ML size on MRI versus CBCT-A showed a higher correlation of the measurements on CBCT-A than on MRI (Tables 3, 4).

Grading of the depth of the OCL lesion on CBCT-A versus MRI was unchanged in 26 patients (Table 5). We noted an upstaging in 5 patients and a downstaging in 3 patients with CBCT-A compared to MRI. There was 1 patient in which the depth was not assessable on MRI. With a p value of 0.12 there was no statistically significant difference between MRI and CBCT-A for this variable.



Coronal Intermediate-W MRI image

Coronal reformatted CBCT-A image

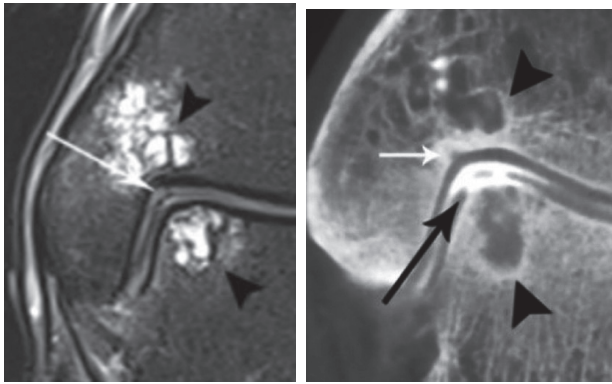
Fig. 2. Example of downstaging of an OCL on CBCT-A compared to MRI. There is BME (white asterisks) at the superomedial aspect of the talar dome. The overlying cartilage is however difficult to assess on MRI, but seems to be slightly inhomogeneous (white arrow). The CBCT-A images reveal complete integrity of the cartilage layer although some subtle subchondral sclerosis (black arrow) is present at the superomedial aspect of the talar dome. This is in line with a non-recent lesion (several months of ankle pain after trauma), indicating healing on CBCT and minor residual BME.

Regarding the degree of detachment, our study showed a statistically significant difference between MRI and CBCT-A with a p-value of 0.003 (Table 6). There was an upstaging of the degree of detachment in 16 patients on CBCT-A. Four patients upstaged from no detachment on MRI to a partial detachment on CBCT-A, whilst 2 patients even upstaged from no detachment on MRI to complete detachment on CBCT-A. A partial detached lesion was upstaged to a complete detached lesion in 10 patients (Fig. 1). There was only one case in which the degree of detachment was downstaged on CBCT-A.

BME was observed in 34 of the 35 patients. On CBCT-A, 33 out of these 35 patients showed focal subchondral bone sclerosis (Fig. 2). The kappa coefficient for this variable was 0.803, proving a high level of agreement between both imaging modalities.

Fourteen patients were diagnosed with subchondral cyst formation on MRI versus 16 on CBCT-A. A kappa coefficient of 0.884 indicates that this imaging parameter has also a high level of agreement between both imaging modalities (Fig. 3). The maximal size of the cysts varied from 2 mm to 15.5 mm.

Additional cartilage lesions of the talus or tibia were present in 8 patients on MRI and in 10 patients on



Coronal Intermediate-W PD MRI image

Coronal reformatted CBCT-A image

Fig. 3. Subchondral cyst formation. Multilocular subchondral cysts are seen on MRI at the distal tibia and at the medial aspect of the talar dome (black arrowheads). The cartilage at the medial talar dome is slightly irregularly delineated (white arrow). There is also a doubtful cartilage lesion at the distal tibia. The coronal reformatted CBCT-A image of the same patient clearly shows an extensive cartilage lesion down to bone with adjacent cartilage flap at the medial aspect of the talar dome (black arrow). The talar and tibial subchondral cysts (black arrowheads) are clearly visualised on this image with a peripheral sclerotic rim. Note also partial filling of subchondral cysts in the talus and tibia with contrast as sign of joint communication through a cartilage lesion.

CBCT-A (Table 7). No additional lesions were found on the articular side of the fibula. There was no statistical significance between MRI and CBCT-A for this variable ($p=0.5$).

Discussion

An OCL is defined as any damage involving both articular cartilage and subchondral bone. Damage to the cartilage may include a small fissure, flap formation and even delamination. Subchondral bone involvement includes BME, fractures, sclerosis and cyst formation [11]. Following the knee, the ankle and elbow are the most common joints to be affected [1]. The talus is vulnerable, as it has a large articular surface with critical blood supply in vulnerable watershed areas which are exposed to impaired healing and necrosis [12].

The first classification system by Berndt and Harty [13] was reported in 1959, consisting of four stages based on the radiological appearance of the lesions.

Their classification has been the basis for other system and has since then been modified first to CT evaluation and later to MRI evaluation. Several modified classification systems have been proposed correlating MRI with arthroscopic appearance [14]. Nowadays, MRI Staging of OCL is usually done by the Anderson classification [15], which is another modification of the initial Berndt and Harty staging system. We opted for a combination of the modified Anderson classification and the modified Outerbridge classification to include both the cartilage and osseous component of the OCL lesions in our staging. Indeed, the Anderson classification does not take into account isolated cartilage lesions without associated fracture. Furthermore, although BME, which is seen in all stages of the Anderson classification, is frequently present in acute post-traumatic setting, in low grade cartilage lesions and chronic OCL, it may be absent.

There are multiple treatment options for OCL of the talus, depending on the stage of the lesion. Conservative treatment consisting of rest, immobilisation and use of anti-inflammatory medication (NSAIDs) is recommended for Berndt and Harty type I and II lesions and small grade III lesions [13]. The aim of this conservative treatment is to unload the damaged cartilage, so the bone marrow oedema can resolve and necrosis is prevented. Extensive type III and type IV lesions are considered for operative treatment. There is a broad range of surgical techniques but a combination of excision, debridement and bone marrow stimulation (BMS) has the best reported rate of success [16-21]. For larger lesions with a fragment size of 15 mm or more, surgical fixation of the osteochondral fragment is preferred [22]. Osteochondral grafting (with autograft or allograft) is indicated for recurrent or refractory lesions and lesions associated with subchondral cysts [16]. In case of intact articular cartilage, retrograde drilling is the best treatment option [12]. The variety of treatment options underscores that accurate and detailed staging of OCL is important to determine the best treatment strategy. If treated incorrectly, early osteoarthritis of the ankle may develop.

Due to its non-invasive nature and absence of any radiation exposure, MRI is nowadays generally accepted as the initial technique for detection and characterisation of OCL lesions. Besides OCL, MRI also allows to evaluate concomitant soft tissue abnormalities. However, due to its higher spatial resolution, the cartilage can be

far better differentiated on CBCT-A, which has previously been demonstrated in a study comparing MRI and CT-A [23]. In our institution, we evaluated the strength of CBCT-A in evaluating OCL of the talus, because CBCT may have some advantages over CT for this indication (**Table 8**) [24].

Our study does not show any statistically significant difference for the size or depth of the lesion on MRI versus CBCT-A. However, CBCT-A led to a more confident reading of the size of the lesions for both readers. There is less inter-rater variability between the measured AP and ML size on CBCT-A than on MRI for both the senior and junior radiologist. The intra-rater variability for measuring the size is more pronounced for the junior than the senior reading, which may be attributed to the level of experience.

Regarding the depth of the cartilage defect of the OCL, distinct grade 4 lesions were equally graded on both imaging modalities, whereas grade 1 and 2 lesions were differently graded on CBCT-A compared to MRI in 6 patients. This suggests that the precise grading of lower grade lesions is more difficult on MRI.

The degree of detachment is the only imaging variable for which our study showed a statistically significant difference between MRI and CBCT-A. There was an upstaging of the degree of detachment in 16 patients. The combination of higher spatial resolution and intra-articular injected contrast which outlines the detached cartilage from the parent bone allows a more accurate assessment. As the degree of detachment correlates with instability of an OCL, this is an important parameter for defining the most appropriate treatment regime [25]. There was only one patient in our study with a downstaging of the degree of detachment on CBCT-A. As this patient was lost in follow-up, there is no arthroscopic correlation.

BME was present in almost all patients on MRI. There is a high level of agreement for the presence of BME on MR or sclerosis on CBCT-A. Although BME is histopathologically different from bone sclerosis, they may both represent two time-dependent responses of bone marrow to trauma. This is in line with the fact that most patients presented in the subacute setting (after several weeks or even months following trauma) at the time reactive sclerosis may have been developed, while BME was not completely resolved on MRI. In one patient without BME, sclerosis was present, which was

attributed to a lesion of older date (5 to 6 months) in which BME had been completely replaced by reparative sclerosis.

Subchondral cyst presence is the other parameter with a high level of agreement on both imaging modalities. Cyst formation may represent an indirect sign of an overlying full-thickness cartilage defect, through which joint fluid may migrate and accumulate into the subchondral bone. In this scenario, CBCT-A may demonstrate filling of the subchondral cyst through the cartilage defect as a direct sign of grade 4 full thickness cartilage defect. The presence, location and size of subchondral cysts have also been previously reported as important criteria for optimal treatment planning. The presence of subchondral cyst formation is also a prognostic indicator with negative impact on the clinical score post-surgery. In addition, the size of the cyst is also important for the treatment strategy, as larger cystic lesions (≥ 8 mm) will require other surgical techniques, namely cartilage replacement [26-29].

Additional cartilage lesions of the talus or tibia were present in 10 patients on CBCT-A versus only 8 patients on MRI. This supports the hypothesis that CBCT-A has a higher sensitivity for detection of OCL than MRI.

Twelve patients underwent surgical treatment of whom 11 were diagnosed with a grade 4 lesion. CBCT-A resulted in an upstaging of the OCL in 7 of these patients needing surgery. Due to limited data of the operative diagnosed degree of the OCL, no detailed arthroscopic correlation was possible. In addition, the decision to operate the patient was taken on a combination of clinical information and imaging findings. Only one patient with a grade 0 OCL on imaging needed surgery with bone grafting of a high grade lesion due to persistent and aggravating ankle pain 24 months following imaging. The discrepancy between the imaging findings and the arthroscopy findings may be explained by a potential lesion progression between the time of imaging and arthroscopy. Thirteen patients were treated conservatively, 5 refused or postponed the suggested surgical treatment of high grade lesions and 5 patients were lost in follow-up post imaging. Of these 5 patients, 4 were diagnosed with a grade 0 to 2 OCL and 1 with a grade 4 lesion on imaging.

Our study demonstrates that compared to MRI, CBCT-A resulted in a significant upstaging of the degree of detachment as well in detecting additional cartilage lesion

in 2 patients. Overall CBCT-A allowed a more confident and intuitive reading with less intra- and inter-reader variability. However, as the technique needs intra-articular contrast injection, it is more invasive. Moreover, it exposes the patient to radiation. Therefore, we propose conventional MRI as screening method if an OCL lesion is suspected. In addition, MRI allows comprehensive evaluation of any concomitant ligamentous and tendon lesions of the ankle joint. In selected cases, where arthroscopic treatment of an OCL is considered, CBCT-A may be useful for more precise preoperative staging and may help the surgeon to decide whether to operate or not.

The strength of our study is its prospective design. A subsequent CBCT-A examination was performed within a time span of maximal 4 weeks following MRI. This avoids significant progression of the lesion between both examinations. Furthermore, all patients were scanned on the same 1.5 T system with a uniform standardised imaging protocol. The limitations of our study are firstly the limited number of patients and secondly the selection bias. The patients were selected based on the MRI characteristics, i.e. the presence of BME and/or cartilage lesion. This excludes patients with a normal MRI, that might theoretically have presented with an OCL visualised only on CBCT-A. A third limitation is the absence of surgical correlation in all patients. A fourth

and last limitation is the magnetic field strength of 1.5 Tesla. The accuracy of the grading also depends on the strength of the field and is lower on 1.5 Tesla magnets in comparison to 3T [30].

Conclusion

We recommend conventional MRI as screening method for osteochondral lesions of the ankle. Additional CBCT-A is reserved for selected cases in which a more accurate cartilage staging is needed in case surgical treatment is considered. CBCT-A is particularly useful for precise evaluation of the degree of cartilage detachment. **R**

Acknowledgement

We would like to thank Kristien Wouters for the statistical assistance for our article.

Funding

This project did not receive any specific funding.

Ethical approval

Medical Ethical Committee, AZ Sint-Maarten, Mechelen, Belgium.

Conflict of interest

The author declared no conflicts of interest.

REFERENCES

- Durur-Subasi I, Duru-Karakaya A, Yildirim O. Osteochondral lesions of major joints. *Eurasian J Med* 2015; 47(2): 138-144.
- Van Dijk N, Reilingh M, Zengerink M, et al. The natural history of osteochondral lesions in the ankle. *Instr Course Lect* 2010; 59: 375-386.
- Van Bergen C, Gerards RM, Opdam K, et al. Diagnosing, planning and evaluating osteochondral ankle defects with imaging modalities. *WJO* 2015; 6(11): 944-953.
- Pirimoglu B, Ogul H, Polat G, et al. The comparison of direct magnetic resonance arthrography with volumetric interpolated breath-hold examination sequence and multidetector computed tomography arthrography techniques in detection of talar osteochondral lesions. *Acta Orthop Traumatol Turc* 2019; 53(3): 209-214.
- Kirschke JS, Braun S, Baum, T et al. Diagnostic value of CT arthrography for evaluation of osteochondral lesions at the ankle. *BioMed Research International* 2016 doi: 10.1155/2016/3594253.
- Schmid MR, Pfirrmann CW, Hodler J, et al. Cartilage lesions in the ankle joint: comparison of MR arthrography and CT arthrography. *Skeletal Radiology* 2003; 32: 259-265.
- Cerezal L, Llopis E, Caga A, et al. MR arthrography of the ankle: indications and technique. *Radiol Clin North Am* 2008; 46(6): 973-974.
- De Smet E, De Praeter G, Verstraete KL, et al. Direct comparison of conventional radiography and cone-beam CT in small bone and joint trauma. *Skelet Radiol* 44(8): 1111-1117.
- Anderson IF, Crichton KJ, Grattan-Smith T, et al. Osteochondral fractures of the dome of the talus. *J*

- Bone Joint Surg Am* 1989; 71(8): 1143-1152.
- 10 Outerbridge R. The etiology of chondromalacia patellae. *J Bone Joint Surg Br* 1961; 43: 752-757.
 - 11 Posadzy M, Desimpel J, Vanhoenacker FM. Staging of osteochondral lesions of the talus: MRI and Cone Beam CT. *J Belg Soc Radiol* 2017; 101(S2): 1.
 - 12 Steele JR, Dekker TJ, Federen AE, et al. Osteochondral lesions of the talus: Current concepts in diagnosis and treatment. *Foot & Ankle Orthopaedics* 2018; 1-9.
 - 13 Berndt L, Harty M. Transchondral fractures (osteochondritis dissecans of the talus). *J Bone Joint Surg* 1959; 41: 988-1020.
 - 14 Hepple S, Winson IG, Glew D. Osteochondral lesions of the talus: a revised classification. *Foot Ankle Int* 1999; 20(12): 789-793.
 - 15 Anderson IF, Crichton KJ, Grattan-Smith T, et al. Osteochondral fractures of the dome of the talus. *J Bone Joint Surg Am* 1989; 71(8): 1143-1152.
 - 16 Badekas T, Takvorian M, Souras N. Treatment principles for osteochondral lesions in foot and ankle. *Int Orthop* 2013; 37(9): 1697-1706.
 - 17 Zengerink M, Struijs PA, Tol JL, et al. Treatment of osteochondral lesions of the talus: a systematic review. *Knee Surg Sports Traumatol Arthrosc* 2010; 18: 238-246.
 - 18 Emre TY, Ege T, Cift HT, et al. Open mosaicplasty in osteochondral lesions of the talus: a prospective study. *J Foot Ankle Surg* 2012; 51(5): 556-560.
 - 19 Verhagen RA, Struijs PA, Bossuyt PM, et al. Systematic review of treatment strategies for osteochondral defects of the talar dome. *Foot Ankle Clin* 2003; 8(2): 233-242.
 - 20 Hannon CP, Ross KA, Murawski CD, et al. Arthroscopic bone marrow stimulation and concentrated bone marrow aspirate for osteochondral lesions of the talus: a case-control study of functional and magnetic resonance observation of cartilage repair tissue outcomes. *Arthroscopy* 2016; 32(2): 348-349.
 - 21 Rico JV, Dalmau A, Chaqués FJ, et al. Treatment of Osteochondral lesions of the talus with bone marrow stimulation and Chitosan-Glycerol phosphate/blood implants. *Arthrosc Tech* 2015; 4(6): 663-667.
 - 22 Van Bergen CJA, De Leeuw PAJ, Van Dijk CN. Treatment of osteochondral defects of the talus. *Rev Chir Orthop Reparatrice Appar Mot* 2008; 94(8): 398-408.
 - 23 Kirschke JS, Braun S, Baum T, et al. Diagnostic value of CT Arthrography for evaluation of osteochondral Lesions at the ankle. *Biomed Res Int* 2016; 2016:3594253.
 - 24 Posadzy M, Desimpel J, Vanhoenacker F. Cone beam CT of the musculoskeletal system: clinical applications. *Insights Imaging* 2019; 9 (1): 35-45.
 - 25 Rungprai C, Tennant JN, Gentry RD, et al. Management of osteochondral lesions of the talar dome. *Open Orthop J* 2017; 11: 743-761.
 - 26 Morvan G, Busson J, Wybier M. Tomodensitométrie du pied et de la cheville. *Paris, Masson*, 2003; 87-127.
 - 27 Prado MP, Kennedy JG, Raduan F, et al. Diagnosis and treatment of osteochondral lesions of the ankle: current concepts. *Rev Bras Ortop* 2016; 51(5): 489-500.
 - 28 Easley ME, Latt DL, Santangelo JR, et al. Osteochondral lesions of the talus. *J Am Acad Orthop Surg* 2010; 18(10): 616-630.
 - 29 Deng E, Gao L, Shi W, et al. Both Magnetic Resonance Imaging and Computed Tomography are reliable and valid in evaluating cystic osteochondral lesions of the talus. *Orthop J Sports Med* 2020; 8(9): 1-6.
 - 30 Barr C, Bauer JS, Malfair D, et al. MR Imaging of the ankle at 3 Tesla and 1.5 Tesla: Protocol optimization and application to cartilage, ligament and tendon pathology in cadaver specimens. *Eur Radiol* 2007; 17(6): 1518-1528.



READY-MADE
CITATION

Desimpel J, Vanhoenacker FM. Staging of osteochondral lesions of the talus: comparison of Cone Beam CT - Arthrography with Magnetic Resonance Imaging. *Hell J Radiol* 2021; 6(2): 23-31.